Verification of CFD predictions by Tracer Experiments

Žitný R., Thýn J.
CTU in Prague, FME, Technická 4, 166 07 Prague 6
E-mail: zitny@fsid.cvut.cz, thyn@fsid.cvut.cz

1. Choice and verification of CFD models

There exist lot of similar CFD models implemented in commercial packages and for example the commercial program Fluent 5.3 suggests for modelling of turbulent flows Reynolds Stress Model, standard k-ε and RNG modification of k-ε model, turbulent viscosity transport model Spalart and Allmaras, Large Eddy Simulation and several different models for approximation of boundary conditions at wall. It is not an easy task to decide which of these models is the best for a specific problem. Some of these models are declared as a low Reynolds number models, enabling to predict even the transition from the laminar to the turbulent flow regime, but this prediction is very unreliable. Taking into account also approximation errors, i.e. influence of computational mesh and selected approximation formula it is not surprising that several quite different results of simulations, differing by several tens of percent, are typically obtained.

Example: Let us consider probably the simplest modeling case, flow of incompressible liquid in a smooth pipe (diameter D=100mm, length L=5m), assuming uniform velocity profile at inlet (u=0.1 m/s). The pipe is long enough, so that the velocity profiles as well as the axial gradients of pressure are fully developed at the end of pipe.

The following Fig.1 concerns calculations of pressure drop expressed in terms of friction factor λ_f: Experimentally verified correlation is compared with results obtained by different CFD models, using program Fluent 5.3 (non-uniform grid 50 x 50, 2-nd order upwind approximation of momentum transfer, standard wall functions),

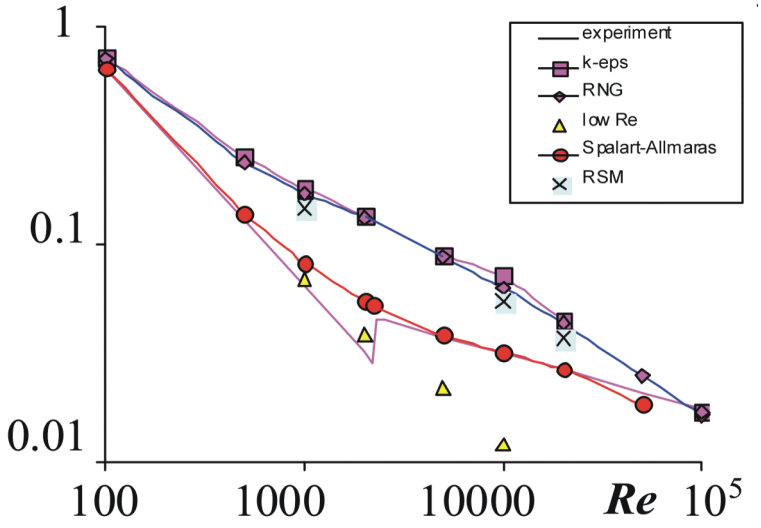

Fig.1 Friction factor λ_f as a function of Re. Fully developed flow in a smooth pipe. Lines denoted as experiment are given by $\lambda_f=64/Re$ in laminar region $Re<2300$, and by $\lambda_f=0.316/Re^{1/4}$ in turbulent region (Blasius).

Appropriate characteristic of radial velocity profile is the ratio of centreline and mean velocity, this ratio is exactly two for ***Re***<2300 while for ***Re***>2300 is much lower, approximately 1.25. see Fig. 2

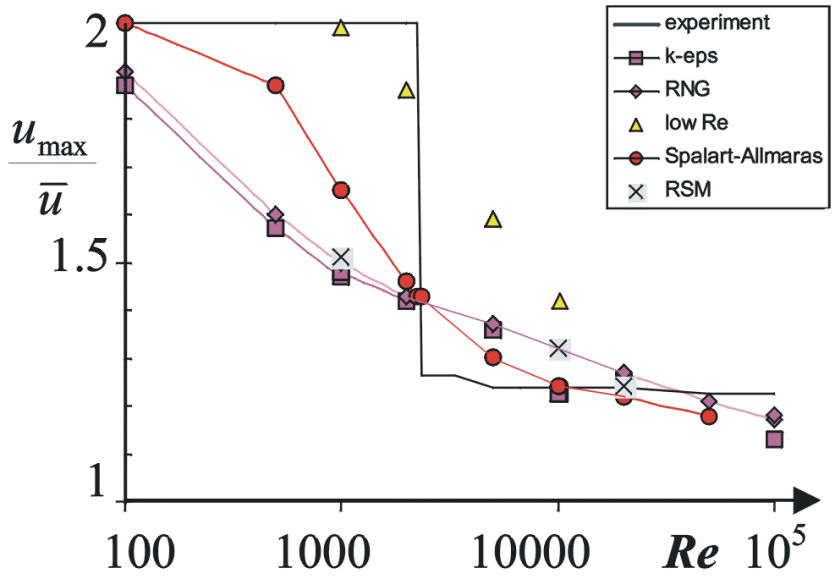

Fig.2 Ratio of maximum and mean velocity of fully developed radial velocity profile in a pipe.

The both figures, 1 and 2, tell the same: CFD models have problems when they are to describe transition between laminar and turbulent regions and the prediction strongly depends upon the model selection. It is surprising but in this simple flow the simplest model, one equation Spalart-Allmaras, is the best. Not knowing the correct solution, the wrong results obtained by standard *k-γ*, RNG and RSM models would be declared as accurate within the broad range of ***Re*** from 100 up to 10^5, because their prediction fairly agrees!

Conclusion: It is nice if the results obtained by different CFD models agree, however only comparison with experiment (or with results obtained by DNS) confirms validity of CFD predictions.

2. CFD and tracer experiments

Local velocities measured by LDA or Pitot tube, pressures, and temperatures are examples of quantities, which can be used for comparison between a CFD model and a real process.

This contribution focuses upon stimulus response technique using tracers. Application of tracer is promising method especially for complicated multiphase flows or for complicated flow structure. Real experiments are typically based on instantaneous injection of a tracer (radionuclide, solution of salt, fluorescent substance and so on) into inlet stream of processed material and monitoring concentration of tracer at outlet (using scintillation detectors, conductivity probes). This impulse response is a time curve $E(t)$, which can be interpreted as the residence time distribution (RTD) of material flowing through the investigated system. This RTD curve is an important integral characteristic of the system itself (prediction of yield of chemical reactions, diagnostics of flow

irregularities, assessment of active and dead internal volumes, and so on, see Thýn (2000)), but at the same time it can be compared with the response predicted by CFD model.

Residence time distributions $E(t)$ can be obtained from calculated velocity field either by particle tracking method or by simulation of stimulus-response experiment, i.e. by solving non-stationary concentration field of a "tracer".

2.1 Particle tracking

The particle tracking explores capability of CFD programs to predict trajectories of dispersed phase particles (the particles must have the same properties, e.g. density, as the continuous phase). The trajectories and residence times are integrated on the basis of known velocity field of continuous phase (Lagrangian method). This approach is straightforward in laminar (convective) flows, on contrary to turbulent flows, where random fluctuations of velocities must be superposed to the mean velocity of continuous phase (discrete or continuous *random walk models*). This provision is necessary, otherwise the injected particles would never enter closed circulation regions (it concerns mass exchange to stagnant regions by diffusion). Magnitude and frequency of these fluctuations are derived from the kinetic energy of turbulence k and the rate of dissipation γ ($u' \approx \sqrt{k}$, frequency $\approx \varepsilon / k$).

2.2 Tracer selection and dosing

Direct simulation of the stimulus response experiment is more demanding from point of view of run-time, because non-stationary solution of continuous phase is to be performed. Stimulus function is usually prescribed as a short pulse or a step change of tracer concentration at inlet, and the corresponding mass-averaged concentrations of tracer at outlet is the residence time distributions $E(t)$, or integral distribution $F(t)$ respectively. Using the impulse instead of the step change of tracer dosing should be preferred because the tracer is usually injected as a short pulse in industrial experiments, and besides this the residence time distribution $E(t)$ is a better characteristic of the system than $F(t)$, as the $E(t)$ is more sensitive to the system behavior.

The simplest way, how to define the pulse in a CFD model is to "patch" the concentration of tracer at or near the inlet zone as an *initial condition*, however this is the *wrong method of dosing* as soon as the velocity at inlet is not constant, see Fig.3

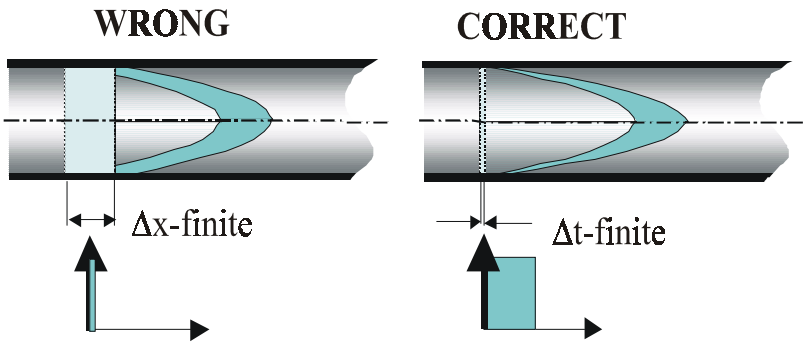

Fig.3 How to define a stimulus function (dosing of "tracer" at inlet). Patching concentrations as ***initial*** *conditions (left) and concentration specified as time dependent* ***boundary*** *conditions (right).*

In the case, that the dosing is prescribed as an initial condition the response is slightly distorted, while in the case that the same amount of tracer is introduced into the system by prescribing time dependent boundary condition at inlet, the response at outlet will be the correct residence time distribution $E(t)$. To prove this, let us consider laminar flow of a Newtonian liquid in a pipe with fully developed parabolic velocity profile. Assuming purely convective mass transfer of tracer, the response (mass averaged concentration of tracer at a cross-section of pipe at a distance L from inlet) is proportional to $\sim 1/t^2$ and $\sim 1/t^3$ in the first (initial) and the second (boundary condition) case respectively, see Thýn (2000). Only the second case is correct because the true residence time distribution is given by

$$E(t) = \frac{\bar{t}^2}{2t^3}, \quad \text{for } t > 0.5\bar{t} \qquad (1)$$

where $\bar{t}$ is the mean residence time. Therefore the monitored response $E(t)$ should be a function decreasing with the third power of time and this requirement is fulfilled by the dosing prescribed as a boundary condition, while the dosing realized as initial condition predicts much slower decrease of concentration at outlet (only as the second power of time).

Duration of the stimulus pulse should correspond to the real experiment, nevertheless precise match is not necessary because only shapes of *normalized* responses are used for comparison of CFD results and experiments. Common recommendation is that the width of pulse should not exceed 3% of mean residence time.

Tracer selected for experiment and the CFD model need not be the same. Probably the best way is to simulate experiment literally, e.g. by modeling of two component mixture of water and tracer (this approach will be used in most examples presented in this contribution). However, for one-phase isothermal flows, it is possible to use *temperature changes* as a tracer if the thermal diffusivity is specified correctly, and if the walls are perfectly insulated. This method was used e.g. for the RTD prediction in the gas flow through the electron beam irradiator, Thyn (1998).

No matter what kind of tracer is used in a CFD model, the correct diffusivity of tracer must be specified (thermal or mass diffusivity). The influence of molecular diffusion of tracer upon predicted residence time distribution is shown in Fig.4.

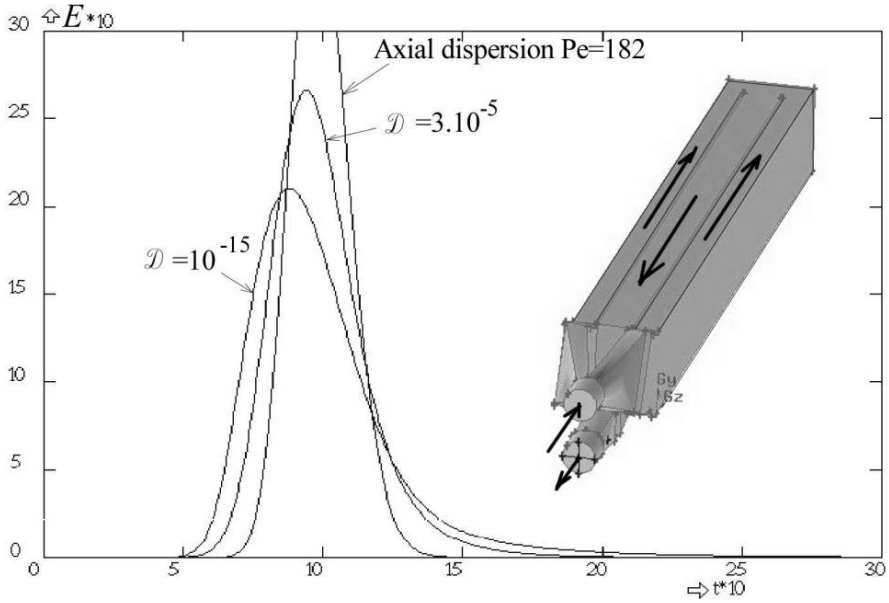

Fig.4 Impulse response of ohmic heater (impermeable electrodes). Fluent 5.3, 250000 tetrahedrons. Time step 1s, mean residence time 114 s. Working liquid water at 20^0C, tracer-water. Flowrate 35.3 ml/s, Re_{inlet}=1500, $Re_{heating\ zone}$=654. Diffusivity $D=3.10^{-5}$ $m^2.s^{-1}$ (narrow response), and $D=10^{-15}$ (wider response). Impulse response of axial dispersion model for corresponding Pe=182 is presented just for comparison.

These results demonstrate the fact that suppressing diffusion (D→0) increases dispersion D_a! This is typical for laminar flows; for example axial dispersion D_a in laminar flow in pipes is related to the diffusion coefficient D according to Taylor (1953) as

$$D_a = \mathrm{D} + \frac{\bar{u}^2 D^2}{192\mathrm{D}} \qquad (2)$$

The third impulse response in Fig.4 was calculated from the simple model of axial dispersion for Peclet number ($Pe=uL/D_a$) corresponding to the given case and dispersion given by Eq.(2) ($D_a=10^{-4}$ $m^2.s^{-1}$). It is obvious that the actual apparatus is characterized by higher dispersion than the equivalent straight circular pipe (with the same length and cross-section) - this is not surprising because the flow-field in heater is not quite simple and there are small dead regions at bottom. However, this difference is of the same order as the difference corresponding to the CFD prediction which neglects molecular diffusion.

2.3 Case study – Direct ohmic heater

2.3.1 Experiments

Numerical modeling and experiments were tested on continuous **direct ohmic heater**, shown in Fig.5. The reason why this continuous heater has been selected for tracer experiments lies in the fact, that the flow pattern – counter current parallel flows – is frequently encountered in apparatuses (not only heat exchangers but also for example core annulus flow pattern in cracking units).

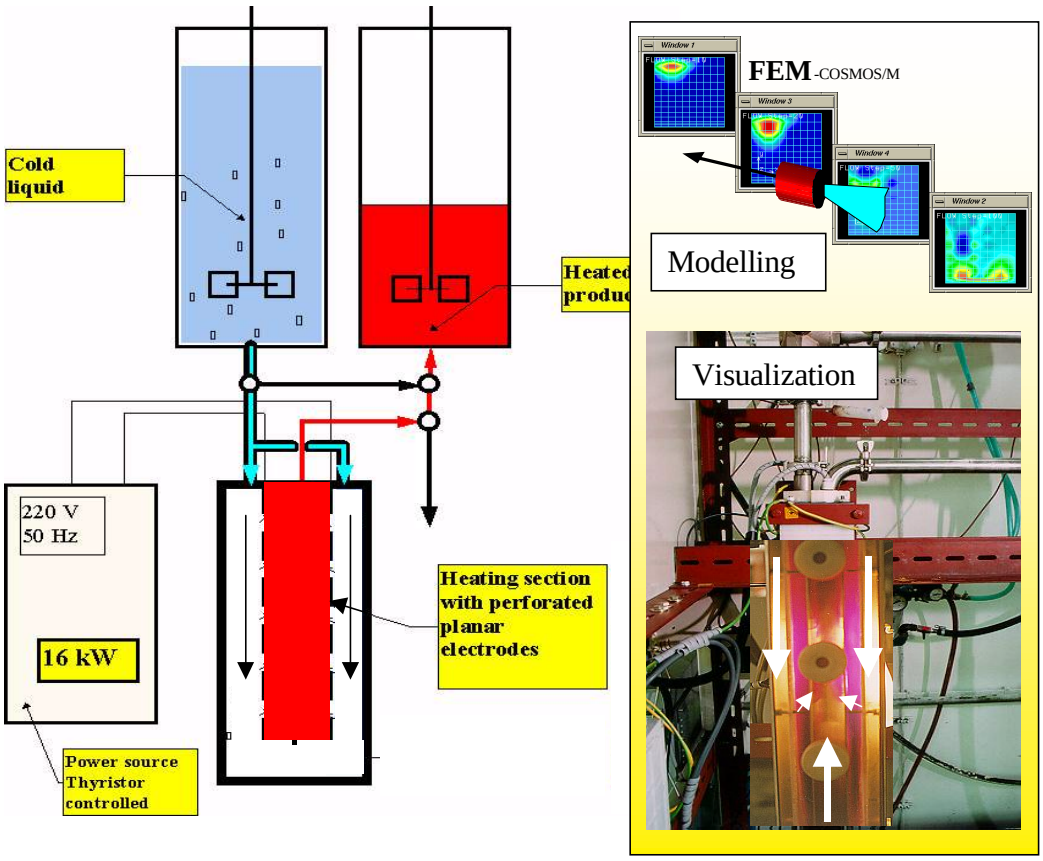

Fig.5 *Direct ohmic heater. Liquid flows towards the bottom in lateral channels (preheating), where the flow is reversed and liquid flows upwards through rectangular heating channel between planar electrodes. What is specific: Electrodes can be perforated thus allowing a part of cold liquid in lateral channels flows directly to the central channel.*

Experimental measurement of RTD by conductivity method used a KCl solution as a tracer. Experimental set-up is in Fig.6.

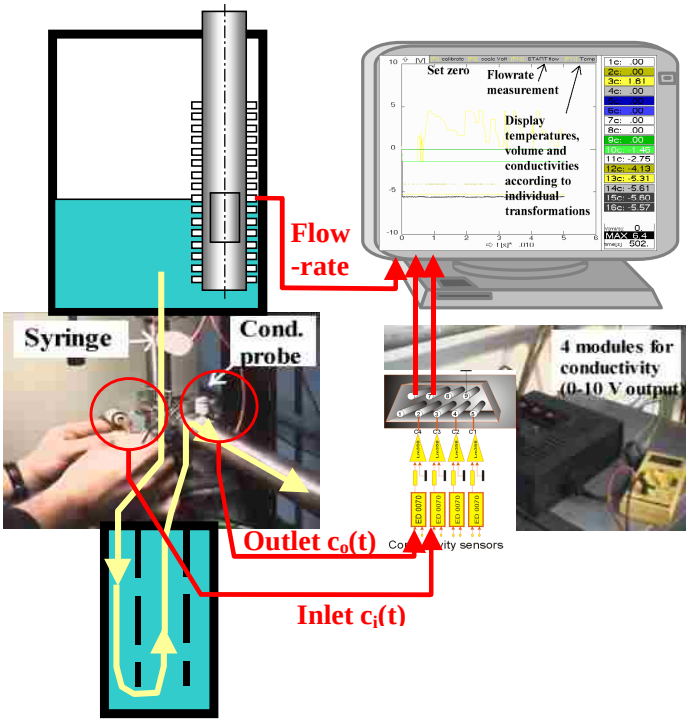

Fig.6

Experimental determination of impulse response. Tracer (water solution of KCl) is injected by a syringe. Time courses of conductivity measured by two Pt probes (located at inlet and outlet) and flow-rate are recorded and evaluated by PC.

Examples of results performed with perforated electrodes are presented in

Tab.1 and Figs. 7, 8 (repeated experiments has been done with the aim to verify the influence of gravity flow if the density of tracer is different than the density of water). It seems that the influence of gravity flow due to different density of tracer is negligible (mass fractions of KCl in water solution 0.056 and 0.028).

Tab.1 Experiments with water and perforated electrodes (data Kareš (1999))

Experiment	Tracer KCl	Flowrate	T [C]	t-mean [s]	σ^2 [-]	t-first [-]
MERENI1	C+56.5g/l	82.4	14	48.14	0.147	0.13
MERENI2	C+56.6g/l	80	13.4	42.95	0.144	0.13
MERENI3	56.5 g/l	89.4	13	43	0.138	0.13
MERENI4	56.5 g/l	91	12	47.8	0.14	0.13
MERENI5	28.25 g/l	89	12.2	44.1	0.147	0.13
MERENI6	28.25 g/l	78	12.2	47.7	0.15	0.13
COSMOS		72		**43.48**	**0.109**	**0.4**
FLUENT		40		**155 (tail)**	**0.568**	**0.1**

Experiments used $KMnO_4$ (potassium permanganate) as a colour marker, and visualisation confirmed previously obtained results: cross-flow through the slits of perforated electrode has character of a jet, penetrating into the main stream, see Fig.7. This cross-flow explains the initial plateau region of impulse response, see Fig.8.

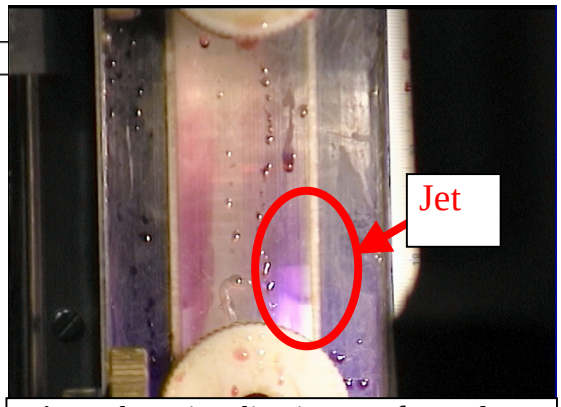

Fig.7 *Flow visualisation, perforated electrode. Flow-rate 80 ml/s.*

Fig.8 *Impulse responses after FFT deconvolution, normalised to unit area. Exponential tail extrapolation. Time step 1 s. Response eEi corresponds to MERENIi in Tab.1*

2.3.2 CFD models of direct ohmic heater

Flow pattern in the heater was analysed by FLUENT 5.3, using 3D model Zajíček (1999). All details of perforation of electrodes were considered, see Fig. 9.

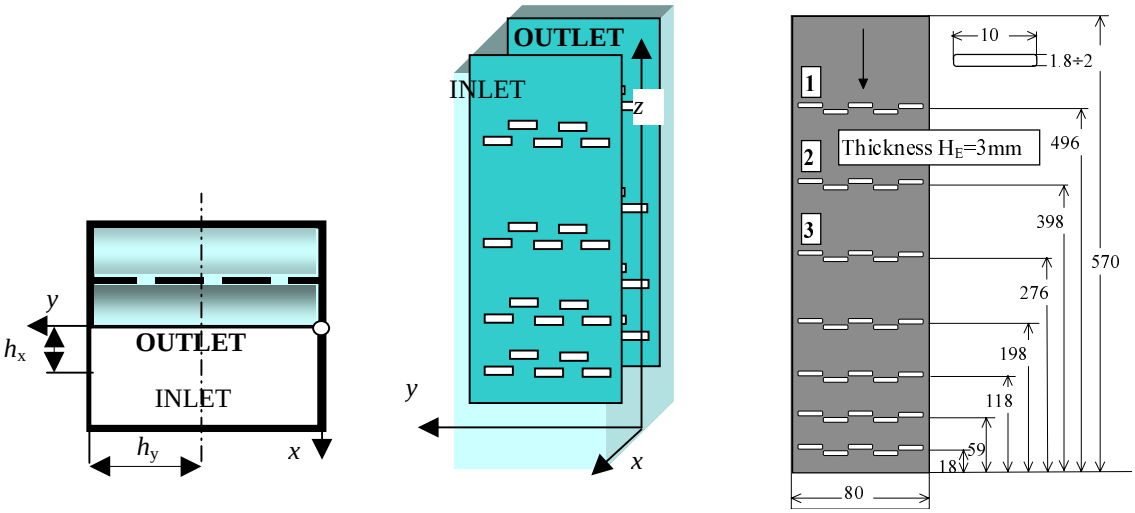

Fig.9 *Geometry of electrodes. Model Fluent 5.3.*

This model has 614348 nodal points. FLUENT calculated evolution of concentration field of the water 2, replacing initial content of heater (water 1) during 178 seconds from start up flow at a constant flow-rate 40 ml/s (constant time steps 2 seconds). In order to calculate the response it is necessary to know the velocity profile at the outlet. Unfortunately this information is missing in ref. Zajicek (1999). Therefore it was assumed that the flow is fully developed at outlet, and the velocity profile was approximated by

$$u(x,y) = \frac{9\dot{V}}{16h_x h_y}[1-(\frac{x}{h_x})^2][1-(\frac{y}{h_y}-1)^2] \qquad (3)$$

The only difference between the FLUENT model and experiments, was flow-rate. Example calculated by FLUENT assumed volumetric flow-rate 40 ml/s, that is nearly two times less than in experiment. Another difference had been in the form of stimulus function: It was not a pulse but a step function 0 – 1, and corresponding response is therefore integral distribution function $F(t)$. However, it is easy to transform the integral distribution into the impulse response, and result is presented in Fig.10.

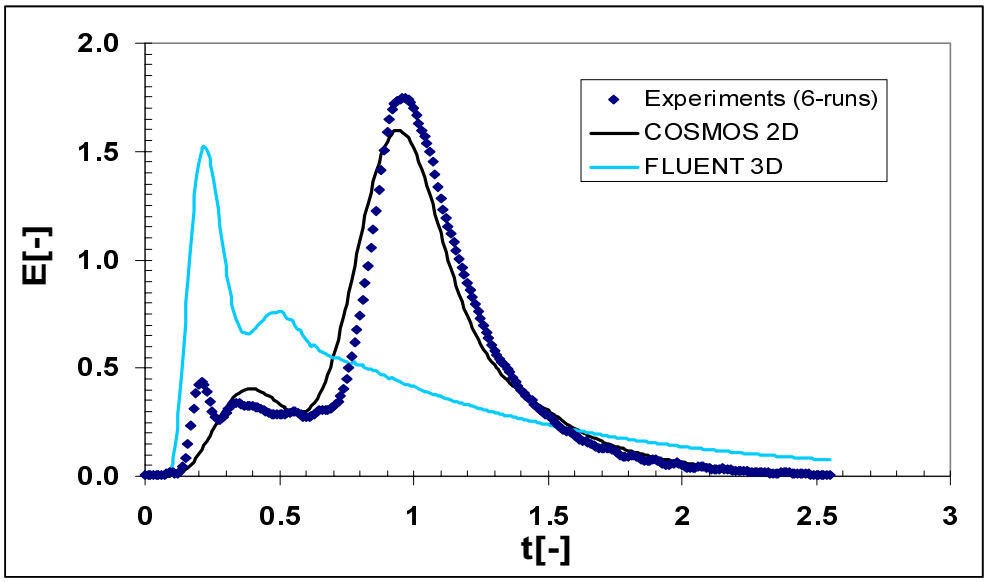

Fig.10 *Dimensionless residence time distributions. Experimental course is average of 6 experiments (Fig.8), COSMOS 2D model having 600 elements, and h=0.028 m (2% time delay was added – substitution of inlet* section*), FLUENT more than 600000 nodes.*

RTD calculated by FLUENT is obviously far from experimentally observed courses $E(t)$, see also Tab.1. This discrepancy cannot be explained only by different flow-rates. It seems that the numerical prediction of the cross-flow through perforated electrodes is overestimated, and even if the numerical mesh is very fine and the flow regime is laminar, the numerical solution is quite unacceptable (though at a first glance it seems to be perfect). Later, after authors of the numerical solution had been informed about experimental results, an effort to improve the CFD model were developed and some errors were really found. New results are presented in Fig.11.

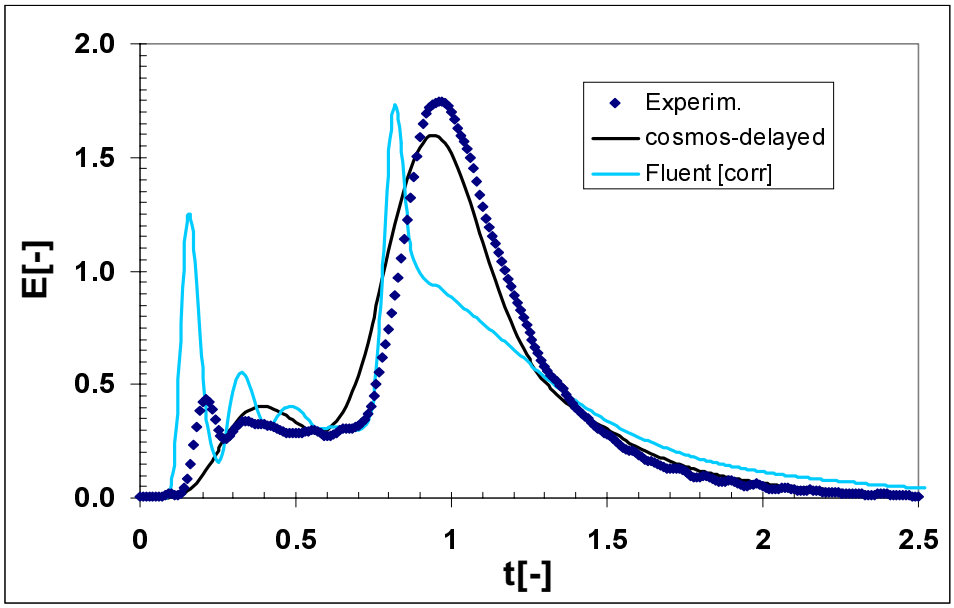

Fig.11 *Dimensionless residence time distributions. The same data as in Fig.10, only the Fluent prediction is corrected.*

This example demonstrates problems encountered in using CFD programs even in seemingly easy situations (laminar flow). It seems that the problems arise from the fact that the CFD model tries to describe relatively large region (height of vessel 0.6 m) and at the same time details describing flow within a narrow gap (0.002 m) – therefore the density of mesh is changing more than hundred times.

In this case it is probably more effective to use only 2 dimensional models, see extremely simplified geometry in Fig.12 (cross-section of heater). For this model the FEM program COSMOS/M, and temperature as a tracer were used.

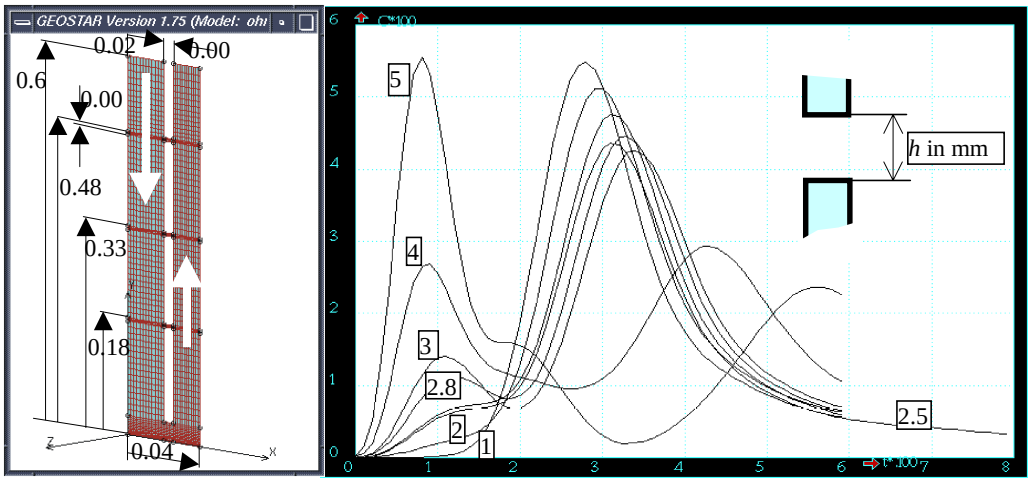

Fig.12 *2D model using COSMOS/M. Impulse responses for different width of slits in electrodes.*

It is not possible to expect fully realistic description of flow field using such a simplified model. However, some geometrical characteristic can be considered as free parameters, which can be identified by comparison of numerical prediction and experimental impulse responses. The width of gaps in perforation h has been selected as the free parameter and several runs were performed for h=1,2,2.5,2.8,3,4,5 mm (actual width was approximately 2 mm). Resulting responses calculated from outlet profiles of temperature and velocity according to Eq.(3) are presented also in Fig. 12.

A high sensitivity of the RTD shape upon the parameter h enables fitting "by eyes". The width h=0.0025 has been selected as the best result, and normalised RTD response has been compared with experimental data and with the prediction by 3D Fluent model in Figs.10, 11. This example demonstrates how experimental results (impulse responses) can be used for development of simplified CFD models.

2.4 Collimated detectors

Tracer experiment need not be restricted to the observation of the input/output signals, and the detectors located near the wall can monitor concentration of tracer at a certain region inside apparatus. Nevertheless, how to interpret signals from such a detector, and what does the detector see? More precisely, what is the relationship between the spatial distribution of tracer and the value given by detector equipped with a collimator?

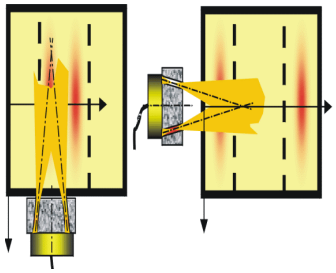

2.4.1 Algorithm of a simple collimator

Given:

- spatial distribution of concentration of a tracer as a general function $c(t,x,y,z)$
- spatial distribution of attenuation as a general function $\mu(t,x,y,z)$ and
- geometry of detector/collimator and their characteristics.

To be calculated:

- detector reading $c_d(t)$.

It is difficult to solve the problem in a general way taking into account all phenomena associated with radiation properties. However, for soft radiation (isotopes of technetium, americium, and so on) the following assumptions can be accepted

- Collimator is an infinite plate of the thickness h having cylindrical hole of diameter d. Material of collimator (e.g. lead) is a perfect absorber of radiation.
- Scattering and reflections can be neglected (this assumption can be approximately satisfied if for example an energy window is used)
- All radiation passing through the collimator hole is catch by detector (100% efficiency).

The question: "What is the intensity of radiation detected by a collimated detector?" is now reduced to a purely geometrical problem, see Fig.13.

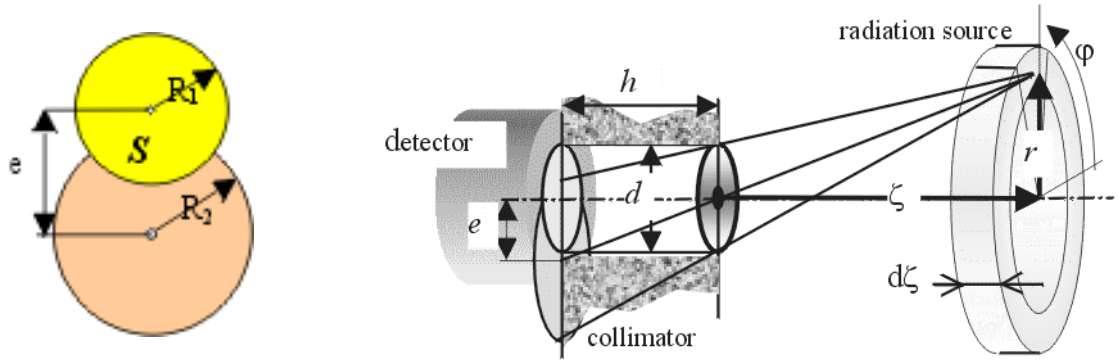

Fig.13 *Collimation (geometry)*

Consider first the hole in collimator aligned with the axis ζ of the cylindrical coordinate system. Area of detector which is irradiated from the point (ζ,r,φ) can be calculated as the intersection of two discs (projection of aperture and the hole) having radii

$$R_1 = \frac{d}{2}; R_2 = \frac{d(h+\zeta)}{2\zeta}, \text{ and distance of centers } \quad e = \frac{hr}{\zeta}. \tag{4}$$

The area of intersection of two overlapping discs equals

$$S = R_1^2 \arcsin\frac{b}{eR_1} + R_2^2 \arcsin\frac{b}{eR_2} - b, \tag{5}$$

$$\text{where } b = \frac{1}{2}\sqrt{4R_1^2R_2^2 - (e^2 - R_1^2 - R_2^2)^2}. \tag{6}$$

Knowing irradiated area S, it is possible to calculate the fraction of radiation emitted by small element of volume $(dV=d\zeta\, dr\, r\, d\varphi)$

$$dJ = \frac{S\zeta}{4\pi(r^2+\zeta^2)^{3/2}} c(t, r\cos\varphi, r\sin\varphi, \zeta) d\zeta \cdot dr \cdot r d\varphi \tag{7}$$

and this contribution has to be integrated within the cone $\zeta \in (0,\infty)$, $r \in (0,\ \zeta\, d/h)$, $\varphi \in (0,2\pi)$.

$$c_d(t) \approx J = \int_0^{\infty}\int_0^{\zeta d/h}\int_0^{2\pi} \frac{S\zeta r}{4\pi(r^2+\zeta^2)^{3/2}} c(t, r\cos\varphi, r\sin\varphi, \zeta) d\varphi \cdot dr \cdot d\zeta \quad . \tag{8}$$

J represents incidence power of radiation passing through the hole under assumption of non-absorbing media. So that the attenuation could be respected numerical integration of radiation intensity decay is necessary:

$$c_d(t) \approx J = \int_0^{\infty}\int_0^{\zeta d/h}\int_0^{2\pi} e^{-\int_0^{\sqrt{r^2+\zeta^2}} \rho\mu dl} \frac{S\zeta r}{4\pi(r^2+\zeta^2)^{3/2}} c(t, r\cos\varphi, r\sin\varphi, \zeta) d\varphi \cdot dr \cdot d\zeta \tag{9}$$

where ρ [kg.m^{-3}] is density and μ [m^2.kg^{-1}] is the attenuation coefficient of absorbing media. The attenuation coefficient is not generally a constant and

depends on energy of radiation. Values, which are relevant for our experiments are summarized in the following table, Storm (1973):

Radiation source.	Energy [MeV], 1/2T [years]	Material Density ρ[kg.m^{-3}]	μ [m^2.kg^{-1}]	a=ρμ [m^{-1}]
Technetium 99.	0.14 MeV	Water, 1000	0.0155	15.5
	2.10^5 years	Steel, 7700	0.018	138.6
Cesium 137	0.511 MeV	Water	0.00896	8.96
	30 years	Steel	0.0077	59.3

Focused collimated detectors, shown schematically in Fig.14, have not been applied in industrial experiments yet, however they are successfully used in medicine. CFD modeling enables assessment of possible advantages (increase of resolution and sensitivity) of focused collimators in a specific apparatus.

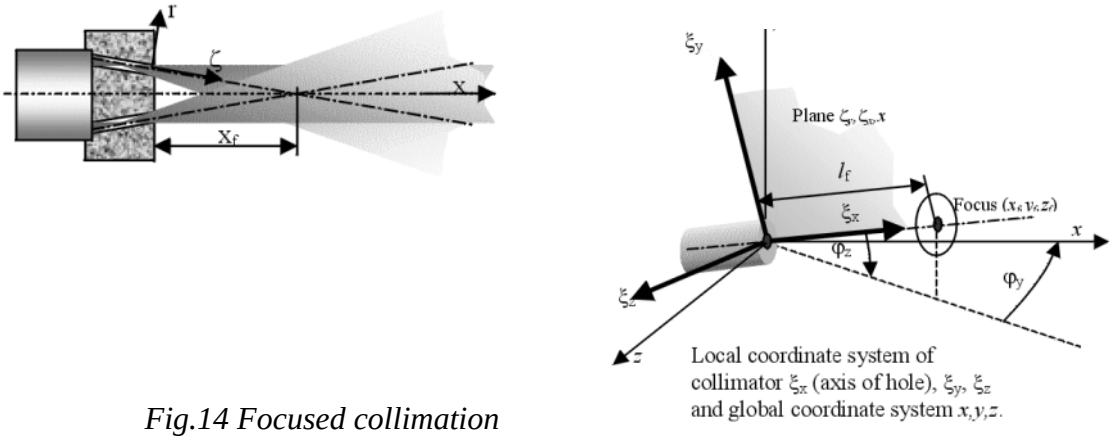

Fig.14 Focused collimation

The same algorithms, i.e. Eqs.(4-9), can be used for focused collimators, only spatial rotations (φ_y,φ_z) must be performed separately for each hole aiming towards the focus, see Fig.14. Rotation φ_z around ζ_z axis merges ζ_y and y axis, and rotation φ_y moves the collimator axis ζ_x to the direction x.

$$x = (\zeta_x \cos\varphi_z - \zeta_y \sin\varphi_z)\cos\varphi_y - \zeta_z \sin\varphi_y$$
$$z = (\zeta_x \cos\varphi_z - \zeta_y \sin\varphi_z)\sin\varphi_y + \zeta_z \cos\varphi_y$$
$$y = \zeta_y \cos\varphi_z + \zeta_x \sin\varphi_z \qquad (10)$$
$$\sin\varphi_z = \frac{y_f}{l_f}, \quad \sin\varphi_y = \frac{z_f}{l_f \cos\varphi_z}$$

where l_f is the focused length and x_f, y_f, z_f are cartesian coordinates of focus.

2.4.2 Processing of CFD data

Let us assume that results calculated by a CFD program has the form of ASCII files from which the following information must be extracted (data filtration):

1. Coordinates of nodal points in cartesian coordinate system (x,y,z). Result is a file, where each row corresponds to one nodal point: i,x,y,z.

2. Connectivity matrix. Group of points forming element or control volume. It is assumed that the element is a "brick" fully determined by eight vertices. Result is a file containing nine integer numbers in each row: i_e, i_1, i_2,i_3, i_4, i_5, i_6,i_7, i_8, where i_e is index of element, and i_j are indices of nodal points (vertices).

3. Calculated vector of concentrations/temperatures at a selected time step. Results are files (one file for each time step) containing pairs i_n, c_n.

These data are used for calculation of detector responses, according to the previously described procedure, see Eqs. (4-10). This algorithm evaluates concentrations of tracer in points x,y,z many times and effectivity of solution depends upon the speed of interpolation $c(t,x,y,z)$ from the CFD data. In the case, that the full list of finite elements is to be searched in order to localise the element containing the point x,y,z, the calculations would be unacceptably slow. Therefore it is necessary to find out a way, how to find out the finite element directly, without necessity to search list of all elements. A possible solution is represented by "cartesian boxing":

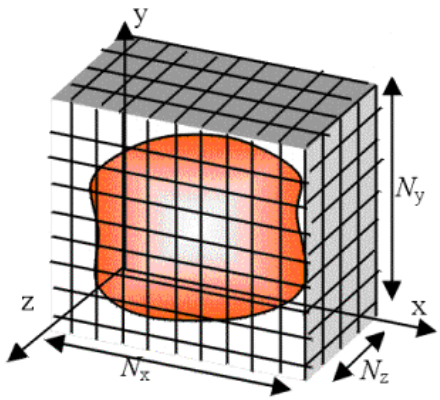

The investigated object (for example the model of heater) is covered by very fine equidistant rectangular grid, consisting of $N_xN_yN_z$ cubes (the size of a cube, h_x, h_y, h_z, should be smaller than the size of the smallest finite element). Now it is possible to find out a mapping between the uniform grid (between centers of cubes) and elements – this procedure is time demanding, however it need to be performed just once, giving matrix $M_{ix,iy,iz}$ whose entries are indices of finite elements. Procedure of identification of finite element is simple:

- Given an arbitrary point x,y,z the indices of mapping matrix M can be idenfified straightforwardly:

$$i_x=int(x/h_x)+1,\ i_y=int(y/h_y)+1,\ i_z=int(z/h_z)+1. \qquad (11)$$

- Value of $M_{ix,iy,iz}$ is the index of finite element containing the box i_x, i_y, i_z and therefore also the point x,y,z.

The second problem is interpolation $c(x,y,z)$ within the selected element (values of concentration at nodes of element are known). This interpolation would be easy for tetragonal elements ($c(x,y,z)=a+bx+cy+dz$), however the

brick with eight nodes is more difficult. There exist the following two more or less standard procedures:

1. Isoparametric transformation, see any standard finite element textbook. This is mapping between the coordinate system in a unit cube (coordinates ξ_1, ξ_2, ξ_3) and coordinate system of element (x,y,z). The transformation explicitly expresses $x(\xi_1, \xi_2, \xi_3)$, $y(\xi_1, \xi_2, \xi_3)$, $z(\xi_1, \xi_2, \xi_3)$, but inverse transformation has to be performed numerically. This inversion need not be done when calculating integrals in FEM (and this is why this form of interpolation is preferred by CFD programs). Unfortunatelly this is not our case, and iterative numerical inversion has to be done.
2. Brick can be split into tetragonal elements and linear interpolation $c(x,y,z)=a+bx+cy+dz$ is used within tetrahedron. However, it is necessary to idenfify the tetragonal subelement containing the point x,y,z and this is also time consuming procedure.

With the aim of simplicity and high performance of interpolation we suggest the following procedure.

1. Calculate distances $l_1,l_2,...,l_8$ between the point x,y,z and nodal points of finite element.
2. Approximate the concentration at x,y,z by formula

$$c(x,y,z)=\frac{\sum_{i=1}^{8}\frac{c_i}{l_i^m}}{\sum_{i=1}^{8}\frac{1}{l_i^m}} \tag{12}$$

where $c_1,...,c_8$ are concentrations in nodes of element and exponent m is dimension of space (1-curve, 2-surface, 3-volume).

Suggested method fullfils the two basic requirements:

- In the case, that the point x,y,z merges with the node j, predicted concentration is c_j.
- If the concentrations $c_1,...,c_8$ are constant, the formula (12) is exact.

Remark: Intepolation (12) reduces to linear intepolation for one dimensional case (m=1) – two node element. $c(x)=\frac{\frac{c_1}{x}+\frac{c_2}{L-x}}{\frac{1}{x}+\frac{1}{L-x}}=c_1(1-\frac{x}{L})+c_2\frac{x}{L}$

Choice of coordinate system.

Global cartesian coordinate system x,y,z can be defined arbitrary, nevertheless from point of view of speed it is convenient to identify x,y,z with the coordinate system, which was

used in the CFD model. Then the positioning of detector (positioning of all holes in collimators) is to be defined also in the coordinate system of the CFD model. For example in our case we shall assume that all detectors are aligned horizontally (y=const): specification of focused collimator geometry is given by point x_c, y_c, z_c (center of front side of collimator), focus length l_f and by the incline of collimator ϑ, see Fig.15

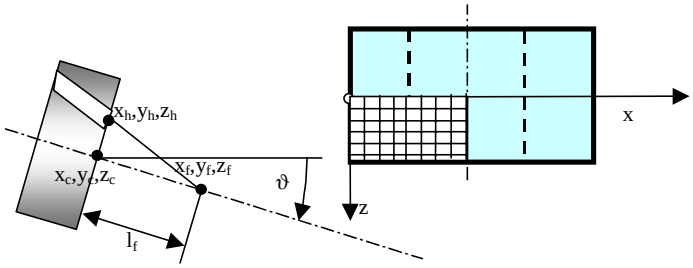

Fig.15 *Geometry of focused collimator with respect to the coordinate system of the CFD model.*

Coordinates of the focus are given by

$$y_f = y_c \qquad (13\text{-}15)$$
$$x_f = x_c + l_f \cos\vartheta$$
$$z_f = z_c + l_f \sin\vartheta$$

Centres of individual holes in the collimator are

$$x_h = x_c + r\sin\varphi\sin\vartheta \qquad (16\text{-}18)$$
$$z_h = z_c - r\sin\varphi\cos\vartheta$$
$$y_h = y_c + r\cos\varphi$$

Example of results is shown in Fig.16, detector looks into the space between electrodes.

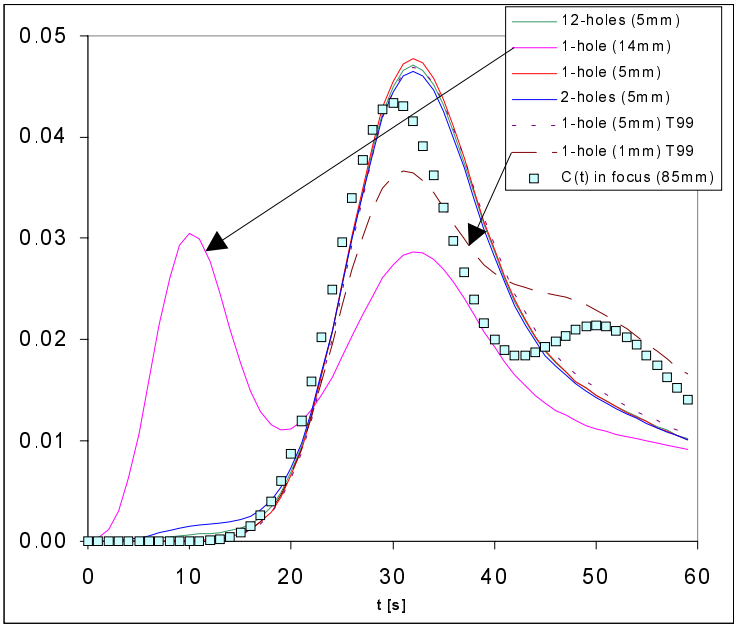

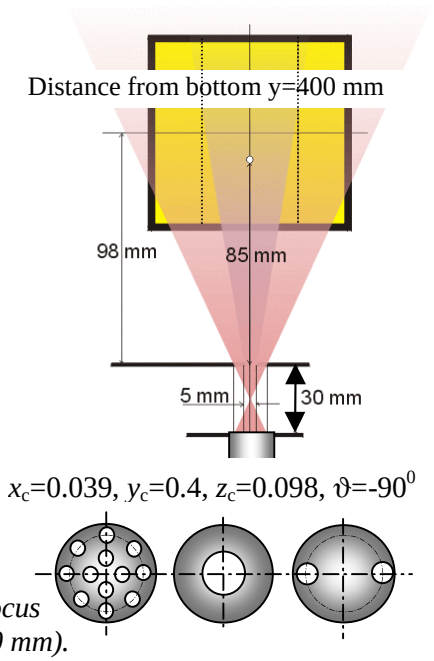

Fig.16 *Detected signal and time course of concentration in focus (l_f=0.085 m, 2,12 holes r=2.5 mm, 1 hole r=1, 2.5, 7mm, h=30 mm).*

The results were calculated for nearly negligible absorption coefficients a_{water}=0.00086 [1/m], a_{steel}=0.0057 [1/m] and also for rather large attenuation a_{water}=15.5 [1/m], a_{steel}=138.6 [1/m], corresponding to 99-Technetium, Storm (1973). Accuracy of solution depends not only upon accuracy of CFD data, and quality of interpolation, but also upon the numerical accuracy of

integration of Eq.(9). Results shown in Fig.16 were integrated using N_x=90, N_r=14, N_φ=17 intervals in ζ,r,φ, cylindrical system of each hole, but nearly the same values were obtained for N_x=60, N_r=9, N_φ=9.

It is seen that the focusing as well as attenuation of radiation has quite negligible effect upon the measured response - the time courses, predicted for one, two, and even twelve holes collimators, are practically indistinguishable. The only important factor is **view angle** – the response, calculated for wide hole collimator (diameter 14 mm, instead of 1 or 5 mm) differs significantly, because the view angle reaches to the lateral channels.

2.4.3 Experiments with focused collimators

Tracer experiments can be substituted by measurements with a sealed radioisotope source either in form of a particle (point source of radiation) flowing inside investigated apparatus, or just only using a point source inside the apparatus in still (without flow). In the second case the experiment yields only information about the actual collimator characteristic and information about absorption and reflection characteristic of the media and internals inside the vessel. These experiments serve not for verification of CFD results, but for verification of the experimental method itself (assumptions, which must be fulfilled if the simplified algorithm of collimation is to be used).

The following Fig.17 and Tab.2 summarise information about location of scintillation detectors D1,..,D4 around the ohmic heater and basic characteristics of collimators, which were used in point source measurements.

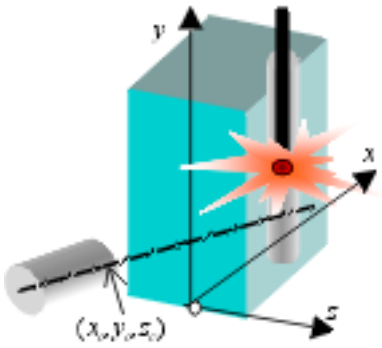

Fig.17 *Point source measurement*

Tab.2. *Positioning of detectors*, Kares (1999)
Horizontal alignment (see Fig.15)

Det.	x_c [m]	y_c [m]	z_c [m]	ϑ [deg]	n-holes(d) [mm]	r_{d1} [mm]	r_{d2} [mm]
D1	0.039	0.125	0.098	-90	1(14)	-	-
D2	0.039	0.400	0.098	-90	12(5)	15	5
D3	-0.067	0.380	0.019	-32.5	1(14)	-	-
D4	-0.067	0.240	0.019	-32.5	8(5)	15	-

Thickness of collim. plate (lead) h=0.03 m
Focus length l_f=0.085 m

By monitoring count rate of the collimated detector at different positions of radiation source (cesium 137), the response function D(x,y,z), corresponding to unit activity at a general point x,y,z can be obtained. The method based on Eq.(12), described in the previous paragraph, can be used for interpolation of N measured points in the three dimensional space, therefore m=3:

$$D(x,y,z)=\frac{\sum_{i=1}^{N}\frac{D_i}{l_i^3}}{\sum_{i=1}^{N}\frac{1}{l_i^3}} \qquad (19)$$

The detector response to a general distribution of activity $c(t,x,y,z)$ can be calculated by integration across the whole volume of apparatus

$$J(y,x,y,z) = \iiint_V D(x,y,z)c(t,x,y,z)dxdydz = \int_0^{2H_x}\int_0^{H_y}\int_{-H_z}^{H_z} D(x,y,z)c(t,x,y,z)dzdydx \qquad (20)$$

The distribution of tracer $c(t,x,y,z)$ in Eq.(20) can be arbitrary and might be obtained for example from CFD calculations.

Theoretical prediction (based upon geometry of collimator D1 and CFD result obtained by COSMOS/M - 3D model without perforation of electrodes) is compared with the response D1 based upon measured D(x,y,z), see Fig.18.

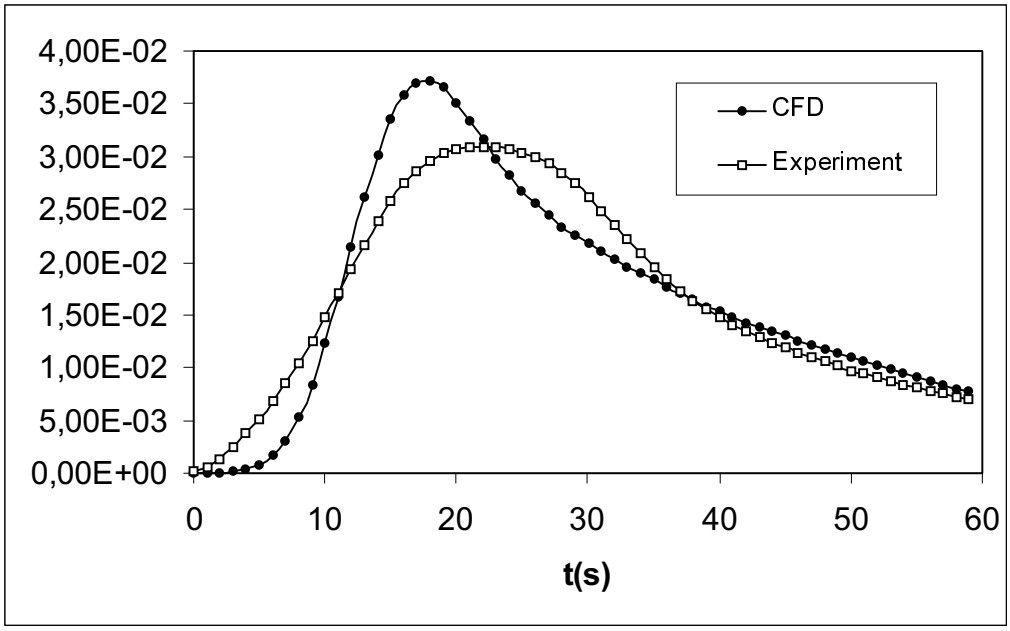

Fig.18 *Time response of detector D1 (1 hole, inclined, y_c=125 mm, x_c=39mm and z_c =98mm), calculated by CFD results at flow-rate 72 ml/s. Comparison of predictions assuming ideal collimation and measured characteristics of detector (sealed source cesium 137).*

It is apparent, that the actual focusing is worse than the theory predicts. This is probably caused by rather high energy of cesium-137 and suggested algorithm of collimation cannot be used with this tracer. We expect that the experiments using technetium could improve collimation characteristics, because the lead collimator is better absorber of low energy radiation.

3. Conclusions:

First part of this contribution concerns evaluation of RTD and more generally the questions about reliability of CFD predictions. It is often believed that the expanding applications of CFD (numerical experiments) make the real experiments obsolete and redundant. However, even such flows, which can be completely mathematically described (e.g. laminar flows using Navier Stokes

equations) can be difficult for CFD modelling and it is not easy to verify correctness of prediction. Experimental verification can be based upon comparison of impulse responses (RTD). It was very surprising, but RTD of direct ohmic heater calculated by extremely fine mesh (Fluent) predicted rather different course (and even the shape) than experiments. Experiments used KCl solution as a tracer and the concentration response was measured by conductivity probes. Experiments were repeated for different concentrations of tracer at the same flow-rate (80 ml/s) and because all responses and identified RTD were nearly the same, the experiment can be considered as reliable. Surprisingly, very simple and only two-dimensional model was able to describe the impulse response rather well. The most important geometrical parameter (width of perforation of electrodes) had to be considered as a free parameter, identified by comparison of impulse response with experiment. However, optimal value of this parameter is close to the actual width, and therefore the simple 2D model seems to be a better description of the flow field, than the complicated 3D model.

Numerical simulation can be a suitable tool for design of experiment and collimation of detectors. This simulation predicts, that the resolution of focused collimators is nearly the same as the non-focused single hole collimators, see Fig.16. While the focused collimators proved to be useful in applications in medicine or for single particle tracking, their disadvantages, first of all significant decrease of sensitivity, would probably prevail in applications with dispersed tracers. On the other hand, the narrow view angle is of a prominent importance as far as the resolution concerns and the multiple-holes collimators, not necessarily the focused collimators, should enable to decrease the view angle without necessity to increase the thickness of collimator.

Numerical modelling of isothermal laminar flow through a continuous heater performed by FEM program COSMOS was used for prediction of detector responses (for different spatial configuration of detectors). The main purpose was validation of algorithms for processing data obtained from the collimated detectors. Instead of experiment at a continuous flow regime with the injection of tracer the following compromise was adopted: Sealed point source of radiation (cesium 137) was inserted into the heater filled by water and responses of four collimated detectors were recorded. Because position of source was changing in all three dimensions, the information about attenuation of radiation D(x,z,y) was obtained. This experimentally identified function D(x,z,y) can be used for prediction of detectors' responses to an arbitrary dispersed tracer within the heater (therefore for an arbitrary velocity field and also for an arbitrary method of tracer injection). This approach (using D(x,y,z)) eliminates errors, caused by differences between actual and numerically predicted concentration fields of tracer. Result of comparison based upon the model of laminar flow without perforation of electrodes is shown in Fig.18. Differences are significant. Possible reasons could be as follows:

1. Suggested algorithms for modelling of collimation or the suggested method of interpolation D(x,y,z) is wrong,
2. Radiation emitted by cesium 137 is too hard. The radiation is not completely absorbed by the collimating plate, so that the assumptions, required by the processing algorithm, are not fulfilled.

Acknowledgement:

This research has been subsidised by the Research Project of Ministry of Education of the Czech Republic J04/98:21220008

List of symbols

c	concentration of tracer	[kg.m^{-3}]
c_d	detected concentration (detector reading)	[count.s^{-1}]
c_{out}	concentration of tracer at output	[kg.m^{-3}]
d	diameter of hole in a collimator	[m]
D	detector reading (response to a unit point source of radiation)	
D	diameter of pipe	[m]
D_a	coefficient of axial dispersion	[m^2.s^{-1}]
e	eccentricity	[m]
E	residence time distribution (impulse response), $E(t)=\mathrm{d}F/\mathrm{d}t$	[s^{-1}]
F	integral distribution of residence times	[-]
h	thickness of collimator	[m]
H_x, H_y, H_z	dimensions of box	[m]
J	radiation power (absorbed by detector)	[W]
l_i	distance between point x,y,z and the nodal point i	[m]
m	dimensionality of space (m=3)	[-]
Pe	Péclet number	[-]
r	coordinate of cylindrical c.s.	[m]
Re	Reynolds number	[-]
S	surface	[m^2]
t	time	[s]
T	temperature	[^{0}C]
u	velocity	[m.s^{-1}]
V	volume	[m^3]
$\dot{V}$	volumetric flowrate	[m^3.s^{-1}]
x,y,z	coordinates of cartesian system	[m]

φ	angular coordinate of cylindrical c.s.	[-]
ϑ	incline of axis of detector with respect to x-axis of global coordinate system	[-]
λ_f	friction factor	[-]
μ	viscosity	[Pa.s]
ρ	density	[kg.m^{-3}]
ξ	axial coordinate of cylindrical coordinate system	[m]

References

1. Kareš J.: Aplikace detektoru záření na identifikaci proudění (in czech). Dipl.thesis, CTU Prague, FME U218, 2000.
2. Kareš J.: Personal communication, CTU Prague 1999
3. Storm E., Israel Ch: Tabulky lineárního hmotnostního součinitele zeslabení, Moskva 1973
4. Taylor T., Reynolds P.W.: The spatial response of course-collimator-detector systems for industrial aplications of computer tomography. Atomic Energy of Canada Ltd., 1984
5. Taylor,G., Dispersion of Soluble Matter in Solvent flowing slowly through a Tube, Proc. Roy. Soc. A, 219, pp.186-203 (1953).
6. Thýn J., Žitný R., Klusoň J, Čechák T.: Analysis and diagnostics of industrial processes by radiotracers and radioisotope sealed sources, Vol.I, CTU Prague, 2000
7. Thýn J., JOON-HA, J., Střasák, P., Žitný R.: RTD Prediction, Modelling and Measurement of Gas in Reactor; Int. Conference CHISA 96 Prague (1996); see also Nukleonika., Vol.43, No.1, p.95-114, (1998).
8. Zajíček M.: RTD- Ohmic heating. CD-ROM, Techsoft Engineering, s.r.o., Prague, 1999